



CHORUS

This is the accepted manuscript made available via CHORUS. The article has been published as:

Strategy for finding a reliable starting point for $G_{\{0\}}W_{\{0\}}$ demonstrated for molecules

Thomas Körzdörfer and Noa Marom

Phys. Rev. B **86**, 041110 — Published 27 July 2012

DOI: [10.1103/PhysRevB.86.041110](https://doi.org/10.1103/PhysRevB.86.041110)

A Strategy for Finding a Reliable Starting Point for G_0W_0 Demonstrated for Molecules

Thomas Körzdörfer¹ and Noa Marom²

1. Center for Organic Photonics and Electronics, Georgia Institute of Technology, Atlanta, GA 30332, USA

2. Center for Computational Materials, Institute of Computational Engineering and Sciences, The University of Texas at Austin, Austin, TX 78712, USA

emails: TKoerzdoerfer@gatech.edu, noa@ices.utexas.edu

Abstract

Many-body perturbation theory in the G_0W_0 approximation is an increasingly popular tool for calculating electron removal energies and fundamental gaps for molecules and solids. However, the predictive power of G_0W_0 for molecules is limited by its sensitivity to the density functional theory (DFT) starting point. We introduce a non-empirical scheme, which allows us to find a reliable DFT starting point for G_0W_0 calculations. This is achieved by adapting the amount of Hartree-Fock-exchange in a hybrid DFT functional. The G_0W_0 spectra resulting from this starting point reliably predict experimental photoelectron spectra for a test set of 13 typical organic semiconductor molecules.

Photoelectron spectroscopy (PES) is one of the most important techniques for probing the electronic structure of molecules and solids, including organic electronic materials. Often, PES measurements are combined with electronic structure calculations. This combination of theory and experiment has been used successfully in the past to gain far-reaching physical insight, regarding e.g., the assignment of PES peaks to particular molecular orbitals, as exemplified by Refs.¹⁻¹⁰

Density functional theory (DFT) in the Kohn-Sham (KS)¹¹ or Generalized Kohn-Sham (GKS)¹² frameworks is currently the method of choice for electronic structure calculations for molecules and solids. When it comes to predicting electron removal energies however, the KS approach suffers from the fact that the interpretation of KS eigenvalues as electron removal energies is formally not based on solid ground. Although exact KS-eigenvalues are approximations to relaxed ionization energies to zeroth order in the adiabatic coupling constant,¹³ only the highest occupied KS eigenvalue has a strict physical meaning, i.e., it equals the first ionization potential.¹⁴ A better approach to calculating electron removal energies and fundamental gaps is to include many-particle effects by employing many-body perturbation theory within the *GW* scheme.^{15, 16} In this approximation the self-energy is obtained from the product of the one-particle Green's function, *G*, and the dynamically screened Coulomb interaction, *W*. Fully self-consistent *GW* (sc*GW*) calculations are very demanding on computational resources, time, and memory, which is why only a handful of sc*GW* results for molecules have been published.¹⁷⁻¹⁹ Instead, a non-self-consistent approach, known as *G₀W₀*, is often used. Using a self-consistent GKS calculation as a starting point, the quasiparticle (QP) energies ϵ_i^{GoWo} are obtained as a perturbative first-order correction to the GKS eigenvalues :

$$\begin{aligned}\epsilon_i^{GoWo} &= \epsilon_i^{GKS} + (1 - b_{HF}) \langle \varphi_i(r) | \hat{v}_x^{HF} - v_x^{KS}[n] | \varphi_i(r) \rangle + \langle \varphi_i(r) | \hat{\Sigma}_c - v_c^{KS}[n] | \varphi_i(r) \rangle \\ &=: \epsilon_i^{GKS} + (1 - b_{HF}) \Delta v_{x,i} + \Delta v_{c,i}\end{aligned}\quad (1)$$

where $\varphi_i(r)$ and ϵ_i^{GKS} are the *i*-th GKS orbital and eigenvalue, respectively, \hat{v}_x^{HF} is the nonlocal Hartree-Fock (HF) exchange operator, $\hat{\Sigma}_c$ is the nonlocal correlation self-energy, $v_x^{KS}[n]$ and $v_c^{KS}[n]$ are the local KS exchange and correlation potentials, respectively, and b_{HF} is the fraction of HF exchange used in the global hybrid functional of the GKS starting point.

The *G₀W₀* scheme has had notable successes in the description of the electronic structure of various organic^{17, 18, 20-22} and metal-organic molecules.^{23, 24} However, the fact that *G₀W₀* is not self-consistent

gives rise to a dependence of the results on the DFT starting point. Recently, a significant G_0W_0 starting point dependence has been observed for molecular systems.^{18, 21-25} For some molecules, shifts of over 1 eV in the QP energies along with major changes in the orbital ordering have been observed when going from one starting point to the other.

Fig. 1 exemplifies the problem. The top curve shows the experimental PES of pyridine²⁶ together with the QP energy spectra (energies convoluted with 0.3 eV Gaussians to simulate the experimental broadening), as obtained from G_0W_0 based on different DFT starting points (these are denoted as G_0W_0 @functional). Clearly, the choice of the DFT starting point significantly influences the quality of the resulting spectra, both in terms of the peak positions and the ordering of the frontier orbitals. For pyridine, the best agreement with experiment is obtained from a starting point of the Perdew-Burke-Ernzerhof (PBE)²⁷ functional, combined with 20% exact (Fock) exchange (denoted as PBE+20%EXX). However, so far no single DFT functional has been demonstrated to be a generally reliable starting point for G_0W_0 . Hence, a systematic and non-empirical approach to find a reliable DFT starting point is clearly needed if one wants to employ G_0W_0 to *predict* and not only to *confirm* experimental spectra. Such a non-empirical scheme is proposed below.

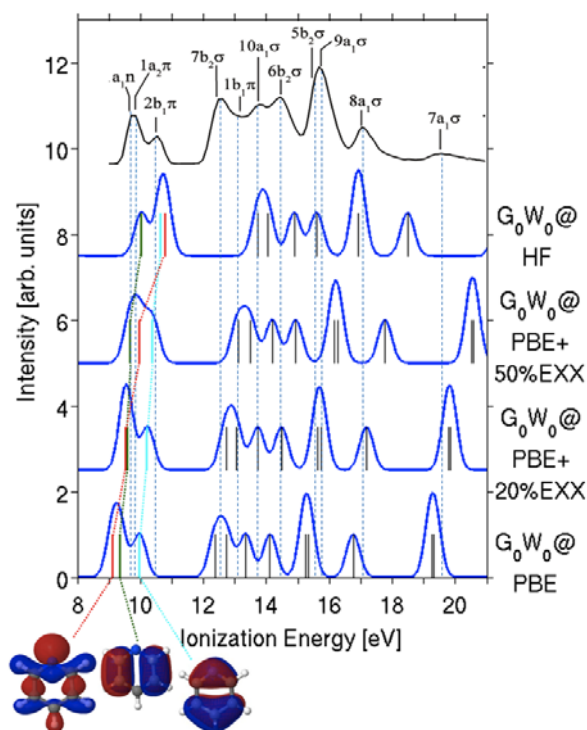


Figure 1: G_0W_0 spectra based on HF and various DFT starting points compared to experimental PES²⁶ for pyridine.

It has been demonstrated that self-interaction errors (SIEs) in semi-local approximations for the exchange-correlation functional can cause severe distortions in the KS eigenvalue spectra.^{6, 23, 28-31} Consequently, severe SIEs in the underlying DFT calculation may cause a significant starting point dependence in G_0W_0 .^{18, 23, 24,32} Specifically for pyridine, the large SIE associated with the highly localized nitrogen lone-pair causes changes in the position of the n -orbital with respect to the π -orbitals (see Fig.1 and Ref. ¹⁸). SIE-free KS-DFT^{10, 11} commonly predicts electron removal energies and orbitals in very good agreement with PES experiments, not only for the orbital energies but also for their character, even for the most challenging systems.⁹ Calculating the so-called “orbital self-interaction error” (OSIE)¹⁸ can therefore help predict if a large starting point dependence for a certain system of interest is to be expected.¹⁸ However, the OSIE does not lead to a systematic way to improve upon the starting point. Moreover, even a SIE-free KS approach is not expected to be an optimal starting point for G_0W_0 : the occupied KS-eigenvalue spectrum cannot be expected to approximate the true QP spectrum for the deep-lying orbitals and, more importantly, the unoccupied eigenvalue spectrum lacks the derivative discontinuity. Hence, if SIE-free KS eigenvalues and orbitals were used as a G_0W_0 starting point, a significant overscreening due to the too small KS gap as compared to the true QP gap would arise. At the same time, starting from the (also self-interaction free) HF eigenvalues would lead to a significant underscreening in G_0W_0 due to a too large eigenvalue gap. Therefore, reducing the SIE in the DFT starting point is only one part of the solution. In order to predict accurate ionization energies from G_0W_0 it is also essential for the DFT starting point to capture the “right amount” of screening.

The use of hybrid functionals within a GKS scheme can help overcome these deficiencies of the KS and HF starting points. GKS eigenvalues mimic the QP corrections to the KS eigenvalues by including a fraction of the exchange-only derivative discontinuity.^{12, 33} In fact, the partial inclusion of $\Delta v_{x,i}$ typically leads to GKS eigenvalues of comparable quality to those from fully SIE-free KS schemes for the occupied spectrum, although the SIE is only partially corrected.³³ Moreover, when it comes to the unoccupied eigenvalue spectrum, the GKS approach has an advantage over the KS description. In contrast to the KS gap, the GKS-gap can indeed equal the fundamental band gap if an appropriate amount of HF-exchange is employed. Typically however, the amount of HF-exchange needed to correct the occupied states (20-25%) is much smaller than that needed to correct the fundamental gap (50-80%). Although this is clearly a severe drawback of standard hybrid functionals, it may turn out as a strength when it comes to finding an optimal starting point for G_0W_0 : it has been argued that a

certain amount of overscreening, induced by a too small gap, is actually desirable to compensate partially for neglecting the vertex correction in the GW approximation.^{18, 34} Consequently, GKS schemes can be expected to be a more promising starting point for G_0W_0 than their KS counterparts.

The primary goal of this work is to provide a non-empirical scheme that generates a generally applicable and consistent GKS starting point for G_0W_0 calculations. Based on eq. (1), it is tempting to search for b_{HF} , such that the GKS eigenvalues are equal to the QP energies, i.e.:

$$\Delta v_{c,i} = (1 - b_{HF}) \Delta v_{x,i} \quad (2)$$

Indeed, for a single orbital, it is possible to find such a fraction of EXX (see e.g., fig. 4 in ref.²⁴). However, different orbitals may require a significantly different b_{HF} . For instance, for magnesium phthalocyanine (MgPc), the a_{1u} orbital, delocalized over the macrocycle, requires 100% EXX, whereas the b_{2g} orbital, localized on the nitrogen lone-pairs, requires 55% EXX (see also supplementary information). Therefore, we search instead for b_{HF} , such that:

$$(1 - b_{HF}) \Delta v_{x,i} + \Delta v_{c,i} \approx c, \quad (3)$$

with c being a constant. If a GKS starting point for which Eq. (3) holds is found, the resulting GKS eigenvalue spectrum may be considered as consistent with the G_0W_0 spectrum, in the sense that the relative orbital energies are correct and the QP correction amounts to a rigid shift of the whole spectrum.

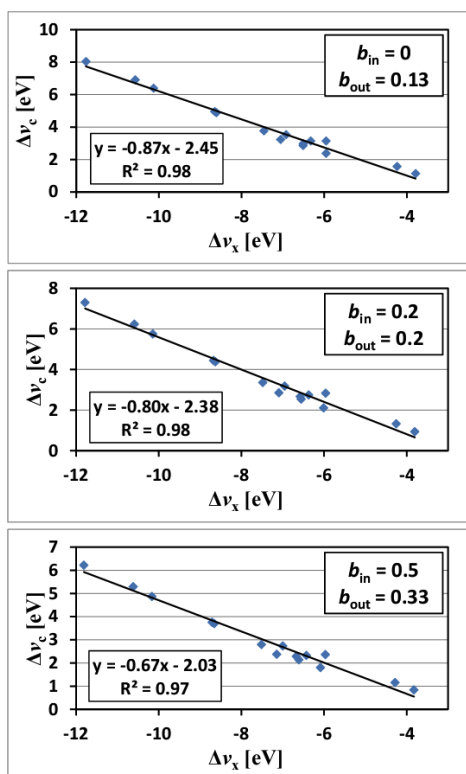
The consistent starting point (CSP) for G_0W_0 can be found by employing the following non-empirical procedure: Start by choosing some semilocal or hybrid DFT method and calculate the corresponding self-consistent (G)KS eigenvalues and orbitals. Then, use this set of orbitals and eigenvalues to calculate $\Delta v_{x,i}$ and $\Delta v_{c,i}$. If Eq. (3) holds, plotting $\Delta v_{c,i}$ as a function of $\Delta v_{x,i}$ should give a straight line. If severe deviations from linearity are found (by calculating the coefficient of determination R^2 of a linear regression), no standard semilocal or hybrid functional is likely to provide a reasonable starting point for G_0W_0 . If a straight line is found, the slope (found from linear regression) should equal $(b_{in}-1)$, where b_{in} is the amount of HF-exchange used in the GKS-starting point standard hybrid functional. If the actual slope of the line, b_{out} , is larger (smaller) than b_{in} , a larger (smaller) fraction of HF-exchange is needed. Following this procedure, a CSP for G_0W_0 can be found without referring to experimental data. This procedure aims to fix the relative energies in the occupied QP spectrum rather than the absolute position of any particular QP energy or the value for the fundamental band gap. It can be viewed as finding a fraction of EXX, which, on average, works best to correct the different OSIE carried by each orbital. Therefore, it is robust and insensitive to the character of any particular orbital.

In the following, it is demonstrated how the proposed scheme helps improve the starting point for G_0W_0 calculations from first principles for a test set of 13 molecules, illustrated in the supplementary information. All calculations were performed using the all-electron numerical atom-centered orbital (NAO) code, FHI-aims.³⁵ Geometry relaxations made use of the PBE functional with a *tier 2* basis set. The implementation of G_0W_0 in FHI-aims is described in Ref.²⁵. G_0W_0 calculations based on PBE with a varying fraction of exact exchange (EXX) were conducted with a *tier 4* basis set, which has been shown to be highly converged, typically to within 0.1 eV from experimental ionization potentials (IP) and electron affinities (EA).²³⁻²⁵ The self-energy was calculated by analytical continuation.

We start our discussion with pyridine. Empirically, a hybrid with 20% EXX is found to yield the best agreement with experiment (see Fig. 1). Following the proposed scheme, we calculate and plot Δv_c as a function of Δv_x for pyridine using the set of eigenvalues and orbitals from the semilocal PBE-functional (see Fig.2). Δv_c (Δv_x) can be well described by linear regression, as indicated by an R^2 -value close to 1. However, the slope of the line predicts a $b_{out}=0.13$ compared to a $b_{in}=0$, indicating that a larger fraction of HF-exchange is needed. Starting the G_0W_0 from a PBE+50%HF hybrid yields a straight line, whose slope yields $b_{out}=0.33$, i.e., the $b_{in}=0.5$ used initially is too large. Only when using PBE+20%HF as a starting point, consistency between b_{in} and b_{out} is obtained, i.e., $b_{in}=b_{out}=0.2$. To provide a quantitative analysis of the improvement reached by the CSP, the mean error (ME)

and mean absolute error (MAE)

in the G_0W_0 spectra



obtained from the different starting points were calculated with respect to the positions of the peak maxima, extracted from the experimental spectrum (see dotted vertical lines in Fig. 1), with N being the number of distinct peaks in the experimental spectra. For pyridine, the MAE is 0.34 eV for the PBE, 0.48 eV for the PBE+50%EXX, and 1.11 for the HF starting point. The MAE calculated from the CSP is 0.14 eV, which is the smallest among all starting points tested and only slightly larger than what is generally considered as the accuracy of the G_0W_0 method itself (0.1 eV). In terms of the ME, the improvement is even more apparent. The CSP yields an ME of +0.02 eV, whereas the MEs for the other starting points barely change as compared to the MAEs (see supporting information). Our non-empirical scheme thus confirms that PBE+20%EXX is a suitable starting point for G_0W_0 for pyridine. It is also worth noting that the change in the slope is mainly due to the change in ϵ . The change in ϵ upon addition of an increasing fraction of EXX is small, which is consistent with the ability to predict the GKS eigenvalues based on a semi-local calculation.³¹

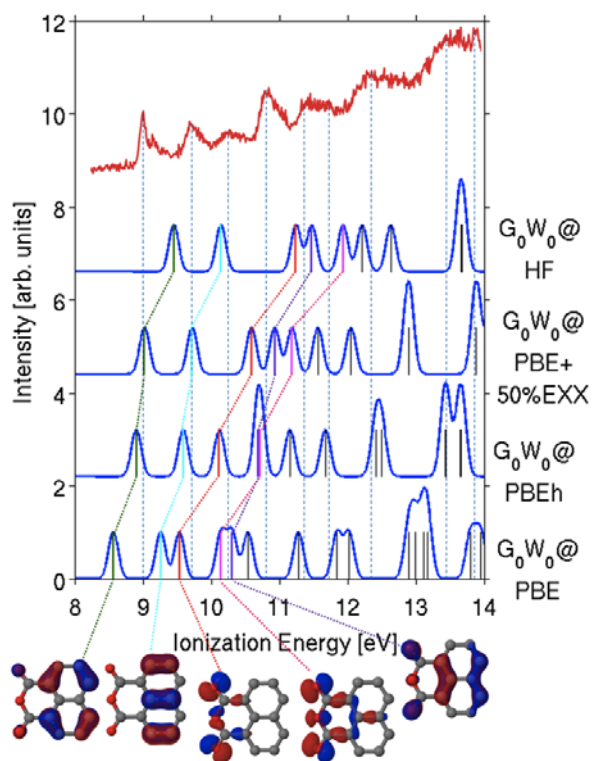


Figure 3: G_0W_0 spectra based on HF and various DFT starting points compared to experimental PES³⁶ for NTDCA.

Table 1: Fractions of exact exchange in a PBE-hybrid for the consistent G_0W_0 starting point for all studied molecules. Chemical structures and plots for the linear regression of $\Delta v_{c,i}(\Delta v_{x,i})$ and comparison to experimental spectra for all molecules are shown in the supplementary material.

Molecule	Pyridine	Benzene	Perylene	Pentacene	NDCA	NTCDA	
b_{HF}	0.20	0.23	0.25	0.25	0.25	0.30	
Molecule	PTCDA	Tetracyanoquino- dimethane (TCNQ)	Tetracyano- ethylene (TCNE)	Benzofurazan	2,1,3-Benzothiadiazol	TTF	MgPc
b_{HF}	0.30	0.24	0.22	0.23	0.18	0.1	0.25

For verification purposes, the above analysis was repeated for *1,8-naphthalene-dicarboxylic anhydride* (NDCA). The curves obtained during the optimization procedure are shown in the supplementary material. Similarly to pyridine, linear regression gives R^2 , which is close to 1. The purely semilocal starting point ($b_{in}=0$) yields a larger $b_{out}=0.18$. The PBE+50%HF starting point ($b_{in}=0.5$) yields a smaller $b_{out}=0.35$. The CSP is found for $b_{in}=b_{out}=0.25$, i.e., PBE+25%EXX, which is known as PBE-hybrid (PBEh or PBE0).^{37, 38} The full comparison of the G_0W_0 spectra obtained from different DFT starting points with experimental PES³⁶ is provided in Fig. 3. Again, the starting point dependence of the G_0W_0 manifests itself both in the absolute QP spectra as well as in the relative orbital ordering. Similarly to *1,4,5,8-naphthalene-tetracarboxylic dianhydride* (NTCDA) and *3,4,9,10-perylene-tetracarboxylic dianhydride* (PTCDA), a large SIE is associated with orbitals localized on the oxygen lone-pairs.^{18,6, 9} These are shifted to lower energies, with respect to the naphthalene-derived orbitals, with the addition of EXX. Again, the analysis of the MAEs as compared to the experimental peak maxima confirms what is apparent from visual inspection of the spectra. The MAE obtained from the CSP is found to be 0.1 eV, thus outperforming the PBE (0.55 eV), PBE+50%HF (0.34 eV), and HF (1.01 eV) starting points.

It is also apparent from Figs. 1 and 3 that the PBE+50%HF starting point slightly improves the IP as compared to the CSP (by 0.1 eV or less). However, this small improvement for the IP comes at the price of significant distortions in the QP spectra, also demonstrated by the large MAE. For the case of pyridine, the PBE+50%HF starting point even predicts the wrong ordering of frontier orbitals: $G_0W_0@CSP$ predicts the highest occupied orbital to have n -character in agreement with experiment, whereas $G_0W_0@PBE+50\%HF$ incorrectly predicts this orbital to have π -character.

Our findings also hold for a set of 11 additional molecules. A complete account of the results, including chemical structure illustrations, $\Delta v_{c,i}$ vs. $\Delta v_{x,i}$ plots, and comparison of the different G_0W_0 spectra to PES,^{26, 36, 39-43} is given in the supplementary material. The b_{HF} values, found to be the CSPs, are summarized in Table 1 for all 13 molecules. They vary between 10% (for tetrathiafulvalene (TTF)) to 30% (for NTCDA and PTCDA). This is in line with the finding that regular hybrid functionals, typically employing 20-25% EXX, work well in many cases. It also means that if the optimization procedure is started from PBEh it is expected to converge in 1-3 G_0W_0 calculations. Based on visual inspection, the CSP yields the best agreement with the experimental spectra for all studied molecules, significantly exceeding the accuracy of $G_0W_0@PBE$ and $G_0W_0@HF$. For most of these molecules, however, a quantitative confirmation of this visual assessment via the MAE is not possible: the experimental peaks are broad, noisy, and may span several energy levels, whose order is not always known. For benzene, one of the molecules for which a clear assignment of energy levels is possible, a MAE of 0.16 eV is obtained from the CSP, again improving upon the PBE (0.39 eV), PBE+50%HF (0.49 eV), and HF (1.07 eV) starting points.

The results presented here confirm the validity of the suggested non-empirical scheme for finding the CSP. The obtained G_0W_0 spectra are in very good agreement with experiments and may thus provide reliable predictions for the valence spectra of systems that are too large for scGW calculations to be feasible (in terms of computer time and memory requirements). In this respect, one may ask how well the optimized G_0W_0 spectra approximate those from scGW. *Specifically*, for pyridine and benzene a comparison of the $G_0W_0@CSP$ spectra to the scGW spectra from Ref. ¹⁸ shows that the $G_0W_0@CSP$ spectra are, in fact, in better agreement with the experiment than the scGW spectra, as confirmed by the significantly larger MAEs of the scGW spectra of 0.31 eV and 0.45 eV for pyridine and benzene, respectively. This finding indicates that, in accordance with earlier observations by others,³⁴ the underestimation of the band gap in the CSP starting point introduces a favorable amount of screening, thus leading to a fortunate cancelation of errors with the omission of the vertex in the self-energy.

In summary, we have introduced a simple and non-empirical scheme for determining a consistent hybrid DFT starting point for G_0W_0 calculations. This is achieved by finding a fraction of exact exchange for which the relative positions of the GKS orbitals are as close as possible to those obtained from G_0W_0 . The G_0W_0 spectra based on the consistent hybrid starting point are in excellent agreement with

PES experiments for a test set of 13 typical organic and metal-organic molecules. By identifying a unique consistent starting point for each system of interest, the proposed scheme yields a practical solution to the problems introduced by the DFT starting point dependence of G_0W_0 . Thus, it extends the range of systems for which reliable predictions of PES spectra from G_0W_0 can be made.

Acknowledgements

The authors thank Fabio Caruso and Xinguo Ren from FHI-Berlin for their interest and help. T.K. thanks the AvH-Foundation for financial support. N.M acknowledges support from NSF grants DMR-0941645 and OCI-1047997, and DOE grants DE-SC0001878 and DOE/DE-FG02-06ER46286. Computational resources were provided by the National Energy Research Scientific Computing Center (NERSC), the Texas Advanced Computing Center (TACC), and the Argonne Leadership Computing Facility (ALCF).

References

1. N. Binggeli and J. R. Chelikowsky, *Physical Review Letters* **75** (3), 493-496 (1995).
2. I. G. Hill, A. Kahn, J. Cornil, D. A. dos Santos and J. L. Brédas, *Chemical Physics Letters* **317**, 444-450 (2000).
3. V. Coropceanu, M. Malagoli, D. A. da Silva Filho, N. E. Gruhn, T. G. Bill and J. L. Brédas, *Physical Review Letters* **89** (27), 275503 (2002).
4. L. Kronik, R. Fromherz, E. Ko, G. Ganteför and J. R. Chelikowsky, *Nature Materials* **1**, 49-53 (2002).
5. C. D. Spataru, S. Ismail-Beigi, L. X. Benedict and S. G. Louie, *Physical Review Letters* **92** (7), 077402 (2004).
6. N. Dori, M. Menon, L. Kilian, M. Sokolowski, L. Kronik and E. Umbach, *Phys. Rev. B* **73** (19), 195208 (2006).
7. N. Marom, O. Hod, G. E. Scuseria and L. Kronik, *The Journal of Chemical Physics* **128** (16), 164107-164106 (2008).
8. G. Stenuit, C. Castellarin-Cudia, O. Plekan, V. Feyer, K. C. Prince, A. Goldoni and P. Umari, *Phys. Chem. Chem. Phys.* **12** (36), 10812-10817 (2010).
9. M. Dauth, T. Körzdörfer, S. Kümmel, J. Zirossoff, M. Wiessner, A. Scholl, F. Reinert, M. Arita and K. Shimada, *Phys. Rev. Lett.* **107** (19) (2011).
10. P. Puschnig, E. M. Reinisch, T. Ules, G. Koller, S. Soubatch, M. Ostler, L. Romaner, F. S. Tautz, C. Ambrosch-Draxl and M. G. Ramsey, *Physical Review B* **84** (23), 235427 (2011).
11. L. J. Sham and W. Kohn, *Physical Review* **145** (2), 561-567 (1966).
12. A. Seidl, A. Görling, P. Vogl, J. A. Majewski and M. Levy, *Phys. Rev. B* **53** (7), 3764-3774 (1996).
13. D. P. Chong, O. V. Gritsenko and E. J. Baerends, *The Journal of Chemical Physics* **116** (5), 1760-1772 (2002).
14. J. F. Janak, *Physical Review B* **18** (12), 7165-7168 (1978).

15. L. Hedin, *Physical Review* **139** (3A), A796 (1965).
16. M. S. Hybertsen and S. G. Louie, *Phys. Rev. B* **34** (8), 5390-5413 (1986).
17. C. Rostgaard, K. W. Jacobsen and K. S. Thygesen, *Phys. Rev. B* **81** (8), 085103 (2010).
18. N. Marom, F. Caruso, T. Körzdörfer, O. Hofmann, X. Ren, J. R. Chelikowsky and P. Rinke, to be published.
19. F. Caruso, P. Rinke, X. Ren, M. Scheffler and A. Rubio, arXiv:1202.3547v1.
20. P. Umari, G. Stenuit and S. Baroni, *Phys. Rev. B* **81** (11), 115104 (2010).
21. X. Blase, C. Attaccalite and V. Olevano, *Phys. Rev. B* **83** (11), 115103 (2011).
22. C. Faber, C. Attaccalite, V. Olevano, E. Runge and X. Blase, *Phys. Rev. B* **83** (11), 115123 (2011).
23. N. Marom, X. G. Ren, J. E. Moussa, J. R. Chelikowsky and L. Kronik, *Phys. Rev. B* **84** (19), 195143 (2011).
24. N. Marom, J. E. Moussa, X. G. Ren, A. Tkatchenko and J. R. Chelikowsky, *Phys. Rev. B* **84** (24), 245115 (2011).
25. X. Ren, P. Rinke, V. Blum, J. Wieferink, A. Tkatchenko, A. Sanfilippo, K. Reuter and M. Scheffler, *New Journal of Physics* **14** (5), 053020 (2012).
26. S. Y. Liu, K. Alnana, J. Matsumoto, K. Nishizawa, H. Kohguchi, Y. P. Lee and T. Suzuki, *J. Phys. Chem. A* **115** (14), 2953-2965 (2011).
27. J. P. Perdew, K. Burke, and M. Ernzerhof, *Phys. Rev. Lett.* **77**, 3865 (1996); *Phys. Rev. Lett.* **78**, 1396 (1997).
28. T. Körzdörfer, S. Kümmel, N. Marom and L. Kronik, *Physical Review B* **79** (20) (2009).
29. T. Körzdörfer, S. Kümmel, N. Marom and L. Kronik, *Physical Review B* **82** (12) (2010).
30. N. Marom and L. Kronik, *Appl Phys a-Mater* **95** (1), 159-163 (2009).
31. T. Körzdörfer, *J Chem Phys* **134** (9), 094111 (2011).
32. W. Nelson, P. Bokes, P. Rinke and R. W. Godby, *Phys. Rev. A* **75** (3), 032505 (2007).
33. T. Körzdörfer and S. Kümmel, *Phys. Rev. B* **82** (15), 155206 (2010).
34. K. Delaney, P. Garcia-Gonzalez, A. Rubio, P. Rinke and R. W. Godby, *Phys. Rev. Lett.* **93** (24), 249701 (2004).
35. V. Blum, R. Gehrke, F. Hanke, P. Havu, V. Havu, X. Ren, K. Reuter and M. Scheffler, *Computer Physics Communications* **180** (11), 2175-2196 (2009).
36. J. Sauther, J. Wusten, S. Lach and C. Ziegler, *J Chem Phys* **131** (3), 034711 (2009).
37. J. P. Perdew, M. Ernzerhof and K. Burke, *J Chem Phys* **105** (22), 9982-9985 (1996).
38. C. Adamo and V. Barone, *J Chem Phys* **110** (13), 6158-6170 (1999).
39. R. Boschi, J. N. Murrell and W. Schmidt, *Faraday Discussions of the Chemical Society* **54**, 116-126 (1972).
40. I. Ikemoto, K. Samizo, T. Fujikawa, K. Ishii, T. Ohta and H. Kuroda, *Chem. Lett.* (7), 785-790 (1974).
41. T. Kobayashi, Z. Yoshida, H. Awaji, T. Kawase and S. Ionedo, *Bull. Chem. Soc. Jpn.* **57** (9), 2591 (1984).
42. J. Berkowitz, *The Journal of Chemical Physics* **70** (6), 2819-2828 (1979).
43. P. A. Clark, R. Gleiter and E. Heilbronner, *Tetrahedron* **29** (19), 3085-3089 (1973).